

1 **An *in vitro* Study to Investigate Biomechanical Responses of Peripheral**  
2 **Nerves in Hypoxic Neonatal Piglets**

3 Anita Singh<sup>a</sup>, Rachel Magee<sup>b</sup>, Sriram Balasubramanian<sup>b</sup>

4 <sup>a</sup>Widener University, Biomedical Engineering, School of Engineering, Chester, PA,  
5 USA

6 <sup>b</sup>Drexel University, School of Biomedical Engineering, Science and Health  
7 Systems, Philadelphia, PA, USA

8 **Corresponding Author & Address**

9 Anita Singh, PhD

10 Associate Professor, Biomedical Engineering,

11 One University Place,

12 Widener University, Chester, PA, USA

13 Telephone: (313)-595-5660

14 Fax: (610)-499-4059

15 E-mail: asingh2@widener.edu

16 Keywords: Neonatal, Brachial Plexus, Stretch, Hypoxia, Injury

17 Short Title: **Hypoxic Neonatal Nerve Responses**

18

19  
20  
21  
22  
23  
24  
25  
26  
27  
28  
29  
30  
31  
32  
33

20  
21  
22  
23  
24  
25  
26  
27  
28  
29  
30  
31  
32  
33

## **Introduction:**

Complex birthing scenarios often lead to prolonged delivery and associated neonatal hypoxia[1–3]. While the adverse effects of neonatal hypoxia on the central nervous system are well studied[4,5,14,6–13], the contribution of hypoxic damage to the peripheral nervous system has not been well investigated. Hypoxia in dorsal roots and ganglions causes abnormal sensations and pain as evident by an increase in firing and decrease in mechanical stimuli thresholds of the tissues[3]. Another study demonstrated long-term effects of neonatal hypoxia evident by persistence of hypomyelination and delayed axonal sorting leading to electrophysiological and motor deficits into adulthood[15]. While these findings strongly support short- and long-term changes in the peripheral nervous system leading to motor impairment post neonatal hypoxia, no studies have reported the effect of hypoxia on the biomechanical properties of neonatal peripheral nerves. A recent study by Bertalan et al., 2020 reported changes in the brain tissue stiffness acutely after hypoxic injury warranting investigation of such injuries on the peripheral nerve, especially in neonates.

An understanding of changes in the neonatal peripheral nerves acutely post-hypoxia can not only help limit peripheral nerve injuries, such as neonatal brachial plexus palsy, but also help understand injury mechanisms and guide the development of timely interventions that limit the hypoxia-induced changes in the neonatal peripheral nerves. This study aims to utilize clinically relevant large animal model (piglet) that has been widely used in neonatal hypoxic and peripheral nerve injury studies, and report changes in the biomechanical properties of hypoxic

neonatal brachial plexus (BP) and tibial nerves.

## **Materials and Methods:**

### **Anesthesia and Surgical Methods:**

All animal protocols were in accordance with NIH Guide for the Care and Use of Laboratory Animals and approved by the Institutional Animal Care and Use Committee. Sixteen neonatal Yorkshire piglets (3-5 days old) were used in this study. Animals were anesthetized and sedated by an intramuscular injection of ketamine (20 mg/kg) and xylazine (1.5 mg/kg). Once sedated, these animals received 4% isoflurane via a snout mask until they reached surgical anesthesia, assessed by the absence of withdrawal response to an in-toe pinch. Piglets were then intubated and maintained on a mixture of 1.5%-2% isoflurane and a mix (50-50) of oxygen and nitrous oxide. Intravenous and arterial lines were also established in the subcutaneous abdominal vein and femoral artery, respectively. Physiological monitoring included non-invasive electrocardiogram (ECG) electrode leads placed on the four extremities, pulse oximeter placed on the skin of the ear to measure oxygen saturation (SpO<sub>2</sub>), and a rectal thermometer to measure core body temperature. A capnometer was attached to the endotracheal tube for end tidal carbon dioxide (EtCO<sub>2</sub>). Arterial blood gases (pH, pO<sub>2</sub>, pCO<sub>2</sub>) were periodically evaluated (every 30 minutes) throughout the experiment. Overall, piglets were continuously monitored, and physiological parameters were collected and recorded every 15 minutes. Anesthetized animals then underwent surgical procedures to expose the BP complex (Figure 1A) bilaterally using an axillary

approach (details outlined in Singh et al., 2019[16]) and tibial nerves using the commonly utilized lateral approach[17].

#### Animal Groups:

All animals were divided into two groups. Normal (n=8) and Hypoxic (n=8). Hypoxia was induced one-hour post-baseline ventilation when normal blood gases and blood pressures were achieved. In hypoxic group,  $\text{FiO}_2$  was decreased to ~7% within minutes (<5 mins) and maintained for an hour. The level of hypoxia was titrated to achieve a target  $\text{PaO}_2$  value of 20 to 24 mm Hg and a minimum 40% reduction in systolic blood pressure from baseline indicating ischemia.  $\text{PaCO}_2$  values were maintained between 35-45 mm Hg. Vital signs were recorded non-invasively every 15 minutes including the heart rate, blood pressure, and temperature. After exposure to hypoxia for an hour,  $\text{FiO}_2$  was returned to normal levels (adapted from Clayton et al., 2017[15]) during which the animals were maintained at normal body temperature of 39°C. Four hours later, the animals were euthanized and their BP and tibial nerves were harvested for biomechanical testing. Normal animals underwent all surgical procedures except induction of hypoxia. The freshly harvested tissues were preserved in 1% bovine serum albumin until biomechanical testing, which was performed within two hours after tissue removal.

#### Biomechanical Test Setup:

A tensile testing machine (eXpert 7600, ADMET Inc., MA) was used to stretch the harvested tissues. Using two clamps, tissue was fixed to the testing device such that one end of the tissue was attached to the fixed end of the machine, and the

other end to the actuator, which was connected to a 200 N load cell (500 series, ADMET Inc., MA) (Figure 1A). Fiducial markers using Indian-ink (shown by two dots on the tissue in Figure 1B) [16, 18] were placed on the tissue to record in situ strain while testing using the high-speed video camera (Basler acA640-120uc camera, PA) that collected data at 120 fps (image resolution: 658x492 Pixels).

#### Testing Procedure:

A digital microscope (Digital VHX Microscope, NJ) was used to obtain images (at 5X) of the harvested tissue and measure the tissue diameter (assuming circular cylinder) at three locations along the entire length of the tissue. The two clamps were initially set at a distance of 20-50 mm (depending on the initial length of the tissue 30-70 mm), and the testing sample was then clamped with no initial tension prior to stretch by visually removing any tissue slack at zero load. The actuator displacement rate was controlled by a built-in GaugeSafe software (Ver. 0.0, ADMET Inc., MA), which applied stretch at a rate of 0.01 mm/s (quasi-static) or 10 mm/s (dynamic) until complete tissue failure occurred. Time, load, and displacement data were acquired during testing at a sampling rate of 1000 Hz. After the completion of the experiment, the failure site was also recorded (example: at or closer to actuator clamp, at or closer to stationary clamp, or along the mid-length of the tissue). Finally, the clamps were checked for presence of any tissue. No tissue inside the clamps implied that the tissue had completely slipped, and data from those experiments were discarded.

#### Data Analysis:

Load data were converted to nominal stresses (i.e. load/original cross-sectional

area of the tissue). Displacement data, obtained from displacement of markers placed on the tissue, were used to calculate tensile strain (i.e.  $\text{Strain} = [(L_f - L_i)/L_i]$ ; where  $L_i$  is initial tissue length,  $L_f$  is final tissue length). The load–displacement and stress–strain curves were plotted, and the maximum load, maximum stress, strain at the point of maximum stress and Young’s Modulus (E). Nerve tissue was assumed to be a homogenous and isotropic material. It exhibited a linear region below the proportional limit of the stress–strain curve. The linear region (based on 20-80% of peak stress) of the stress-strain data was automatically selected using custom-Matlab code and was used to calculate the E. The video data were also used to track changes in structural integrity of the tested samples[18]. As load, displacement and video data were recorded synchronously, the load and tissue strain relationships could be characterized.

#### Statistical Analysis:

At each rate (0.01 mm/s and 10 mm/s), a minimum of 8 samples were tested in both groups (normal and hypoxic) for the neonatal BP and tibial nerves. Statistical analysis, using Independent t-test, was performed using SPSS 27,0 (IBM Corporation, Armonk, NY) to determine the difference in the biomechanical parameters reported in the normal and hypoxic neonatal BP and tibial nerves at the two tested rates (0.01 mm/s and 10 mm/s) and between the two groups (normal and hypoxic).  $p < 0.05$  was considered significant for all tests.

## Results

Out of the 176 brachial plexus segments (chord and nerve), 88 segments were

normal and 88 were hypoxic. Out of the 32 tibial nerves, 16 were normal and 16 were hypoxic. In the normal group, 91% (40/44) of the BP and 88% (7/8) tibial nerves subjected to 0.01 mm/s and 87% (39/44) of the BP segments and 75% (6/8) tibial nerves subjected to 10 mm/s did not slip during testing (Figure 1B). In the hypoxic group, 84% (37/44) of the BP segments and 100% (8/8) tibial nerves subjected to 0.01 mm/s and 82% (36/44) of the BP segments and 88% (7/8) tibial nerves subjected to 10 mm/s did not slip during testing (Figure 1B). Samples that slipped, as evident from the load data and clamping surfaces, were not considered for data analysis.

#### Effects of Hypoxia:

Typical stress-strain responses of normal and hypoxic BP nerves, at both rates, are shown in Figure 2. Similar trends were observed for neonatal tibial nerves. When comparing mechanical properties between normal and hypoxic BP and tibial nerves, significantly lower maximum load, maximum stress and modulus of elasticity (E) in the hypoxic than the normal nerves were observed at both rates (Figure 3). Strain at maximum stress was lower in the hypoxic BP nerves only at the 10 mm/s rate when compared to normal tissue (Figure 3). Failure strains in the normal and hypoxic BP nerves tested at 0.01 mm/s, and normal and hypoxic tibial nerves, at the two tested rates, were not significantly different.

#### Effects of Stretch Rate:

Differences in the mechanical behaviors were observed in the normal and hypoxic BP and tibial nerves when subjected to the two different stretch rates (Figure 3). In both groups, normal and hypoxic, for both tissue, BP and tibial nerves, the



maximum load, maximum stress, and E values were significantly higher ( $p < 0.05$ , independent t-tests) when subjected to 10 mm/s rate than 0.01 mm/s rate. No differences in the strain values were observed in both normal and hypoxic BP and tibial nerves at the two tested rates.

#### Comparing BP and Tibial Nerve:

Normal BP and tibial nerves reported differences in the mechanical behavior when subjected to stretch such that the failure load (only at 0.01 mm/s), stress (both rates) and E (both rates) were significantly higher for tibial nerves than BP nerves. Such differences were not observed in the hypoxic BP and tibial nerve tissues.

#### Failure mode:

During biomechanical tensile testing, the tissue failed either at the actuator end, the fixed end or along the length of the tissue. No significant differences were observed in the occurrence rate of these observed failure location in any tissue among all tested groups.

## Discussion

Human studies in neonates following hypoxia are primarily focused on brain injuries and little is known about the effects of neonatal hypoxia on the peripheral nervous system. Stecker et al., 2013 reported a decrease in nerve action potential in anoxic rat sciatic nerve[19]. Another study by Punsoni et al, 2015[20] also confirmed axonal swelling and disruption of the cytoskeleton in anoxic rat sciatic nerve. A more recent study by Clayton et al., 2017[15] reported neonatal hypoxia in mice to result in hypomyelination and delayed axonal sorting, which further led

to electrophysiological and motor deficits during adulthood. Most recent findings by Bertalan et al., 2020 have reported edema-driven brain tissue stiffening acutely, as early as within five minutes, post-hypoxia in dying brain [21]. These available studies that have reported the effects of decreased oxygenation on the peripheral nerve and other nervous tissue function and structure, both acutely and chronically, support our finding of neonatal hypoxia to affect the biomechanical responses of the peripheral nerves. Although the mechanism responsible for the observed changes were not investigated in this study, serving as a limitation, the current study offers foundational data for future investigations on the biochemical processes responsible for inducing rapid mechanical changes in neonatal hypoxic nerve tissues.

The current study reports the mechanical behavior of hypoxic neonatal BP and tibial nerves at different stretch rates (0.01 mm/s and 10 mm/s) and compare their responses to normal nerves. The chosen rates, representative of quasi-static and dynamic loading conditions, were based on a published study that reported rate-dependent behavior of normal neonatal peripheral nerves [18]. Our findings confirm that hypoxic BP nerves also exhibit rate-dependency. Furthermore, findings from this study indicate that the biomechanical responses of hypoxic neonatal BP and tibial nerves are significantly weaker than normal nerves. Segmental differences between chord and nerve BP tissue could not be performed in this study due to small sample size of the chord segments. Future studies are warranted to investigate segmental differences in BP tissue while utilizing biochemical and structural imaging techniques. These additional techniques could

offer insights into the pathophysiological mechanisms that are responsible for altered biomechanical responses of the hypoxic neonatal peripheral nerves reported in this study.

In the current study, biomechanical responses of hypoxic BP tissue were reported sub-acutely i.e. four hours post hypoxia, under the assumption that changes in the extracellular tissue matrix would have occurred within few hours post-hypoxia. Similar to Bertalan et al., 2020, we also speculated swelling and cytotoxic edema (reported at 1.5 hours post hypoxia) to be responsible for observed tissue stiffening, and thus chose to investigate the biomechanical responses of neonatal BP and tibial nerves four hours post-hypoxia. Future studies, including in-depth biomechanical analysis such as stress-relaxation responses supported by histological and functional analysis, are needed to offer an in-depth understanding of time-dependent changes within the neonatal peripheral nerve post-hypoxia.

In conclusion, the current study establishes that neonatal hypoxia leads to weaker mechanical responses in the brachial plexus. These results also suggest that hypoxia could be a predisposing risk factor for neonatal peripheral nerve injuries, and advancements in neonatal care during complicated delivery encompassing hypoxia warrants greater attention.

## **ACKNOWLEDGEMENTS**

Research reported in this publication was supported by the Eunice Kennedy Shriver National Institute of Child Health and Human Development of the National

240 Institutes of Health (Grant Number R15HD093024), and NSF CAREER Award  
241 (Grant Number 1752513).  
242

## References

- [1] Gilbert, W. M., 1999, "Associated Factors in 1611 Cases of Brachial Plexus Injury," *Obstet. Gynecol.*, **94**(3), p. 483.
- [2] Leung, T. Y., Stuart, O., Sahota, D. S., Suen, S. S. H., Lau, T. K., and Lao, T. T., 2011, "Head-to-Body Delivery Interval and Risk of Fetal Acidosis and Hypoxic Ischaemic Encephalopathy in Shoulder Dystocia: A Retrospective Review," *BJOG An Int. J. Obstet. Gynaecol.*, **118**(4), pp. 474–479.
- [3] Sugawara, O., Atsuta, Y., Iwahara, T., Muramoto, T., Watakabe, M., and Takemitsu, Y., 1996, "The Effects of Mechanical Compression and Hypoxia on Nerve Root and Dorsal Root Ganglia: An Analysis of Ectopic Firing Using an in Vitro Model," *Spine (Phila. Pa. 1976)*, **21**(18), pp. 2089–2094.
- [4] Moral, Y., Robertson, N. J., Goñi-De-Cerio, F., and Alonso-Alconada, D., 2019, "Neonatal Hypoxia-Ischemia: Cellular and Molecular Brain Damage and Therapeutic Modulation of Neurogenesis," *Rev. Neurol.*, **68**(1), pp. 23–36.
- [5] Rocha-Ferreira, E., and Hristova, M., 2016, "Plasticity in the Neonatal Brain Following Hypoxic-Ischaemic Injury," *Neural Plast.*, **2016**.
- [6] Li, B., Concepcion, K., Meng, X., and Zhang, L., 2017, "Brain-Immune Interactions in Perinatal Hypoxic-Ischemic Brain Injury," *Prog. Neurobiol.*, **159**, pp. 50–68.
- [7] Petrashenko, V. A., Loboda, A. M., Smiyan, O. I., Popov, S. V., Kasyan, S. N., Zaitsev, I. E., and Redko, E. K., 2019, "Laboratory Criteria of Perinatal Damage of Central Nervous System at Premature Newborns," *Wiad. Lek.*,

266           **72**(8), pp. 1512–1516.

267   [8]   Torres-Cuevas, I., Corral-Debrinski, M., and Gressens, P., 2019, “Brain  
268           Oxidative Damage in Murine Models of Neonatal Hypoxia/Ischemia and  
269           Reoxygenation,” *Free Radic. Biol. Med.*, **142**, pp. 3–15.

270   [9]   Ruzafa, N., Rey-Santano, C., Mielgo, V., Pereiro, X., and Vecino, E., 2017,  
271           “Effect of Hypoxia on the Retina and Superior Colliculus of Neonatal Pigs,”  
272           *PLoS One*, **12**(4).

273   [10]   Kichev, A., Rousset, C. I., Baburamani, A. A., Levison, S. W., Wood, T. L.,  
274           Gressens, P., Thornton, C., and Hagberg, H., 2014, “Tumor Necrosis  
275           Factor-Related Apoptosis-Inducing Ligand (TRAIL) Signaling and Cell  
276           Death in the Immature Central Nervous System after Hypoxia-Ischemia  
277           and Inflammation,” *J. Biol. Chem.*, **289**(13), pp. 9430–9439.

278   [11]   Anuriev, A. M., and Gorbachev, V. I., 2019, “Hypoxic-Ischemic Brain  
279           Damage in Premature Newborns,” *Zhurnal Nevrol. i Psihiatr. Im. S.S.*  
280           *Korsakova*, **119**(8), pp. 63–69.

281   [12]   Smirnova, A. V., Borzova, N. Y., Sotnikova, N. Y., Malyshkina, A. I., and  
282           Bojko, E. L., 2019, “Method for Predicting Perinatal Hypoxic Lesions of the  
283           Central Nervous System in Newborns,” *Klin. Lab. Diagn.*, **64**(2), pp. 89–93.

284   [13]   Coveñas, R., González-Fuentes, J., Rivas-Infante, E., Lagartos-Donate, M.  
285           J., Cebada-Sánchez, S., Arroyo-Jiménez, M. M., Insausti, R., and Marcos,  
286           P., 2014, “Developmental Study of the Distribution of Hypoxia-Induced  
287           Factor-1 Alpha and Microtubule-Associated Protein 2 in Children’s  
288           Brainstem: Comparison between Controls and Cases with Signs of

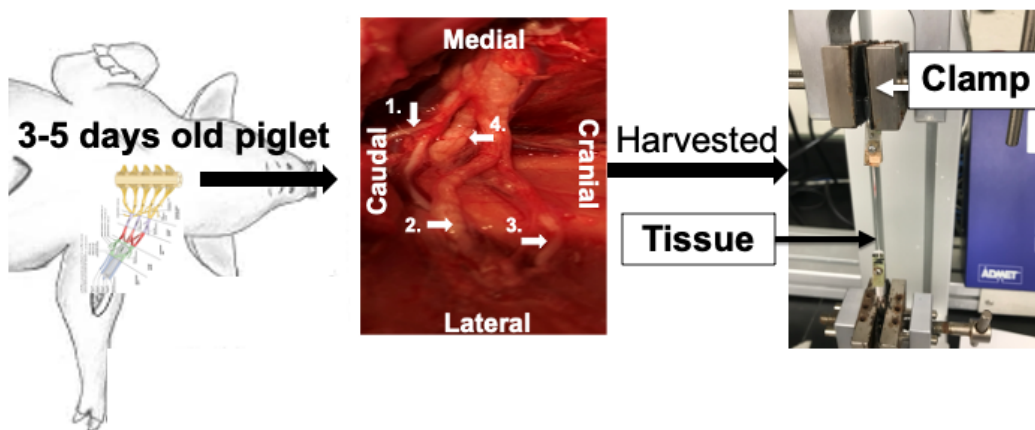
- 289 Perinatal Hypoxia,” *Neuroscience*, **271**, pp. 77–98.
- 290 [14] Studenikin, M. J., 1982, “Fetal and Neonatal Hypoxia,” *Pediatr. Pathol.*,  
291 **17**(2), pp. 271–278.
- 292 [15] Clayton, B. L. L., Huang, A., Dukala, D., Soliven, B., and Popko, B., 2017,  
293 “Neonatal Hypoxia Results in Peripheral Nerve Abnormalities,” *Am. J.*  
294 *Pathol.*, **187**(2), pp. 245–251.
- 295 [16] Singh, A., Magee, R., and Balasubramanian, S., 2019, “Methods for in Vivo  
296 Biomechanical Testing on Brachial Plexus in Neonatal Piglets,” *J. Vis.*  
297 *Exp.*, **2019**(154).
- 298 [17] Zilic, L., Garner, P. E., Yu, T., Roman, S., Haycock, J. W., and Wilshaw, S.  
299 P., 2015, “An Anatomical Study of Porcine Peripheral Nerve and Its  
300 Potential Use in Nerve Tissue Engineering,” *J. Anat.*, **227**(3), pp. 302–314.
- 301 [18] Singh, A., Shaji, S., Delivoria-Papadopoulos, M., and Balasubramanian, S.,  
302 2018, “Biomechanical Responses of Neonatal Brachial Plexus to  
303 Mechanical Stretch,” *J. Brachial Plex. Peripher. Nerve Inj.*, **13**(1), pp. e8–  
304 e14.
- 305 [19] Stecker, M., Wolfe, J., and Stevenson, M., 2013, “Neurophysiologic  
306 Responses of Peripheral Nerve to Repeated Episodes of Anoxia,” *Clin.*  
307 *Neurophysiol.*, **124**(4), pp. 792–800.
- 308 [20] Punsoni, M., Drexler, S., Palaia, T., Stevenson, M., and Stecker, M. M.,  
309 2015, “Acute Anoxic Changes in Peripheral Nerve: Anatomic and  
310 Physiologic Correlations,” *Brain Behav.*, **5**(7).
- 311 [21] Bertalan, G., Klein, C., Schreyer, S., Steiner, B., Kreft, B., Tzschätzsch, H.,

de Schellenberger, A. A., Nieminen-Kelhä, M., Braun, J., Guo, J., and  
Sack, I., 2020, “Biomechanical Properties of the Hypoxic and Dying Brain  
Quantified by Magnetic Resonance Elastography,” *Acta Biomater.*, **101**, pp.  
395–402.

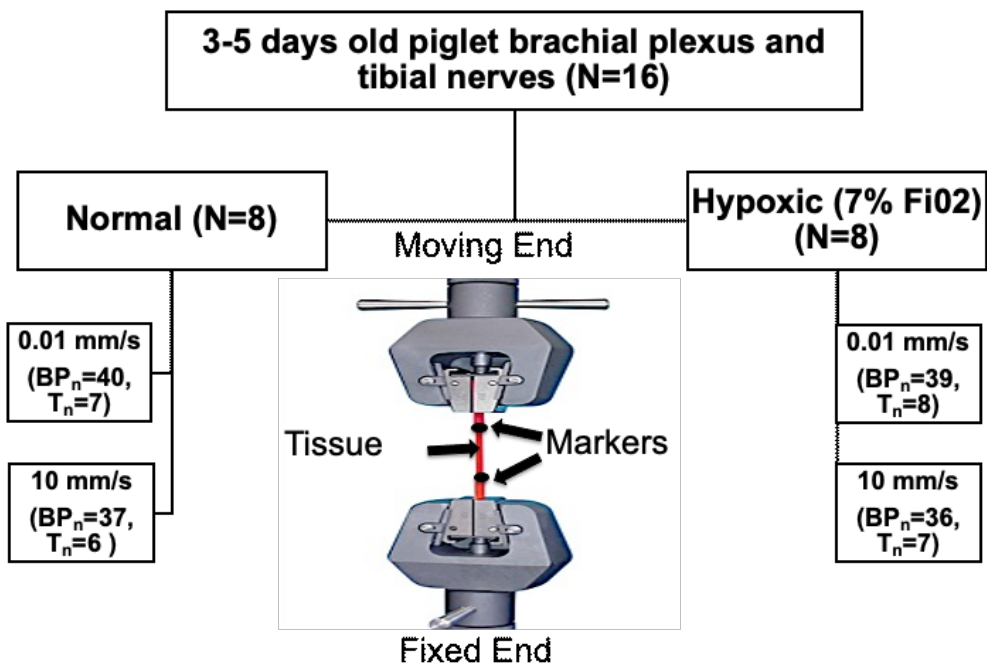


Figure Legends:

Figure 1: A: Experimental details including tested BP nerves (1: Musculocutaneous nerve, 2: Median, 3: Ulnar, 4: Radial) and the tensile testing setup. B: Groups and testing condition details. N: Number of animals per group. BP<sub>n</sub>: Number of BP nerve samples included in data analysis, T<sub>n</sub>: Number of tibial nerve samples included in data analysis.



A:



B:

Figure 2: Exemplar Stress-strain responses from normal and hypoxic neonatal brachial plexus nerve at 0.01 mm/s and 10 mm/s rate.

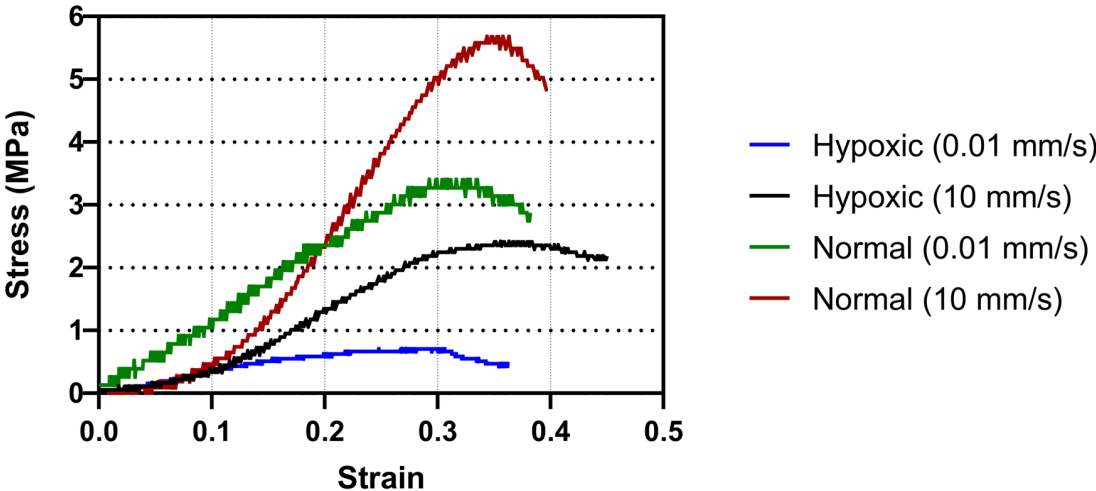


Figure 3: Summary of reported failure responses during tensile testing represented as, A: peak load (N), B: strain at peak stress, C: peak stress (MPa), and D: modulus of elasticity (E) in normal and hypoxic neonatal brachial plexus and tibial nerves at 0.01 mm/s and 10 mm/s rate. Lines above the column represent significant differences between the groups, # represent significant differences between the nerve types and \* indicates significant rate effect with  $p < 0.05$  considered significant.

